metals

MDPI

Article

Experimental SHPB Study of Limestone Damage under Confining Pressures after Exposure to Elevated Temperatures

Lei Liu [1,2], Rui Li [1], Hao Qin [1] and Wei Sun [1,2,*]

[1] Faculty of Land Resources Engineering, Kunming University of Science and Technology, Kunming 650093, China; kgliulei@kust.edu.cn (L.L.); ruili@stu.kust.edu.cn (R.L.); 20172101051@stu.kust.edu.cn (H.Q.)

[2] Yunnan Key Laboratory of Sino-German Blue Mining and Utilization of Special Underground Space, Kunming 650093, China

* Correspondence: kmustsw@kust.edu.cn

Abstract: Studying the dynamic performance of rocks affected by high temperatures is a crucial theoretical foundation of mining engineering design and the construction of deep metallic mineral resources. More importantly, such studies can provide technical support for the green and low-carbon mining of these resources. However, systematic studies on the dynamic mechanical properties of rocks affected by both confining pressure and temperature during the mining of deep metallic mineral resources are lacking. Therefore, systematic research was conducted on the dynamic mechanical properties of limestone under confining pressure after high-temperature treatment, and a corresponding constitutive model was established. In this study, limestones were heated to 200 °C, 400 °C, 600 °C, and 800 °C, and the Split Hopkinson Pressure Bar impact test was conducted with confining pressures of 0.0 MPa, 0.5 MPa, 1.5 MPa, and 2.5 MPa. The test results show that the temperature has a significant effect on the dynamic compressive strength of limestone, and as the temperature rises, the strength tends to first increase and then decrease, reaching the turning point at a temperature of 400 °C. The dynamic compressive strength increases as the confining pressure increases. The constitutive equation of the dynamic damage to limestone under confining pressure after high-temperature treatment is consistent with the test results. Therefore, the established constitutive model can represent the dynamic behavior of limestone, providing a reference for evaluating the dynamic performance of this material, and serving as a theoretical basis for the green and low-carbon mining of deep metallic mineral resources.

Keywords: limestone; high temperature; confining pressure; SHPB; constitutive model

Citation: Liu, L.; Li, R.; Qin, H.; Sun, W. Experimental SHPB Study of Limestone Damage under Confining Pressures after Exposure to Elevated Temperatures. *Metals* **2021**, *11*, 1663. https://doi.org/10.3390/met11101663

Academic Editors: Srecko Stopic and Lijie Guo

Received: 25 August 2021
Accepted: 15 October 2021
Published: 19 October 2021

1. Introduction

With the depletion of shallow mineral resources, the mining depth for extracting underground metallic and non-metallic minerals has been growing [1]. The process of deep mining and construction is challenged by a complicated environment with a high ground stress, high ground temperature, high osmotic pressure, and strong mining disturbances of deep rock mass due to dynamic loads, such as blast waves and machine vibrations [2]. In order to provide a theoretical basis for the green and low-carbon mining of deep metallic mineral resources, it is essential to conduct research on the dynamic properties of rocks under a confining pressure and high temperature [3,4]. For example, shotcrete anchor supporting material and filling materials could be preserved. Recently, the continuous development of the Split Hopkinson Pressure Bar (SHPB) experimental technique has resulted in its wide application to the study of dynamic mechanical properties [5–7] and constitutive equations [8,9] of materials. Li X.B et al. [10] developed a dynamic and static loading test system for rocks at medium to high strain rates, and explored the dynamic mechanical properties of rocks under axial static pressure and confining pressure. Numerous scholars have conducted dynamic mechanical experiments for rocks under

various conditions by utilizing SHPB, and great progress has been made. To research the effects of strain rates on the dynamic strength, deformation properties, and failure modes of rock, Ping Qi et al. [11] carried out numerous dynamic compression tests under passive confining pressure. A large number of experimental studies have shown that temperature has a significant impact on the mechanical properties of rock, which has attracted the attention of many scholars [12]. Li Ming [13] adopted XRD and SEM to research the meso-mechanics of the destruction of coal measure sandstone, and analyzed the impact of the temperature and impact load on the mechanical properties and behavior of the studied rock. Yin Tubing [14] developed a new experimental system and utilized it to conduct SHPB testing on siltstone under the coupling effect of temperature and pressure. The experimental results were used to develop a constitutive model of the rock under the coupling of temperature and pressure and dynamic disturbance. In addition to the influence of high temperatures, the deep rock mass is under triaxial stress in its natural state; the deeper the burial depth, the greater the stress of the surrounding rock, and the related indices of its mechanical properties will be affected accordingly. In the process of deep underground mining and underground engineering construction, the strength evaluation, stability control, and engineering design of an engineering rock mass subjected to high stress from the surrounding rock need to consider not only the physical and mechanical properties of rock blocks, but also the influence of confining pressure on its mechanical properties. Related studies have shown that the mechanical properties of the tested specimens change after confining pressure is applied in the SHPB experiment [15–17]. Therefore, to ensure that the study of the dynamic mechanical properties of rock materials is in line with engineering practice, the influence of confining pressure on these properties should not be ignored.

To date, many studies have been conducted on the dynamic mechanical properties of rock under normal temperature and dynamic coupling conditions, or on the uniaxial dynamic mechanical properties of rock subjected to high temperatures. However, few studies have used constitutive equations, which are more suitable for actual deep rock and soil engineering, to research dynamic mechanical properties under the combined effects of high temperature and confining pressure. As a result, it is necessary to conduct research on the dynamic mechanical properties of rocks affected by high temperatures under confining pressure so as to meet the needs of deep ground geotechnical construction.

In this research, the SHPB system was adopted to carry out dynamic compression experiments on limestone specimens after they were subjected to high temperatures (200 °C, 400 °C, 600 °C, and 800 °C) and different confining pressures (0.5 MPa, 1.5 MPa, and 2.5 MPa).

2. Specimen Preparation and Testing Procedure

2.1. Experimental Equipment

Figure 1 shows the Split Hopkinson Pressure Bar (SHPB) dynamic test system with a confining pressure device for testing the dynamic rock mechanics. The overall system consists of the SHPB test system and confining pressure device.

The Split Hopkinson Pressure Bar (SHPB) dynamic test system used in the experiment is composed of an electronic pulse loading device, incident rod, transmission rod, absorption rod, automatic speed monitoring device, signal acquisition and processing system, and other key components. In order to adjust the shape of the stress wave, the cross-section of the end of the incident rod is gradually changed. The material of the rod is 40Cr alloy steel, which has a Poisson's ratio of 0.2 and a longitudinal wave velocity of 5410 m/s. The diameters of the incident rod, transmission rod, and impact rod are 50 mm, and the lengths are 2400 mm, 1200 mm, and 800 mm, respectively.

Figure 2 shows the confining pressure loading system used in the dynamic mechanics experiment under the condition of confining pressure loading, which is mainly composed of the loading sleeve and the pressure oil pump. The pressure oil pump is used to change

the oil pressure in the loading sleeve so as to adjust the confining pressure applied to the specimen.

Figure 1. SHPB test system.

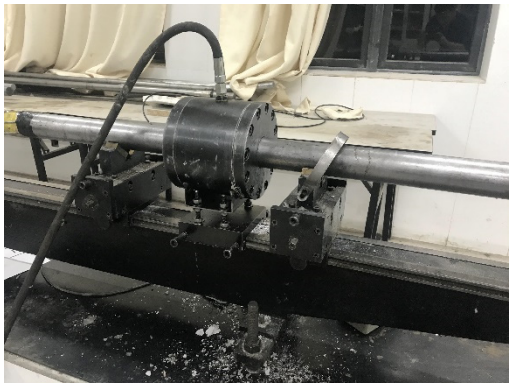

Figure 2. Confining pressure device.

The heating device was manufactured by the Zhengzhou Xinghai Instrument Equipment Co., Ltd., used to heat the limestone specimen. The working voltage of this device is 220 V, and the rated power is 5000 W. The length, width, and height of the working chamber are 300 mm × 200 mm × 120 mm, respectively. The device is welded with high-quality high-temperature-resistant materials, and the maximum controllable temperature is 1200 °C.

After heating the rock for the high-temperature experiment, the storage device uses a WGLL-230BE electric heating blast drying oven made by Tianjin Tester. The working voltage is 220 V; the rated power is 3000 W; and its studio length, width, and height are 600 mm × 500 mm × 750 mm, respectively. The range of constant temperature fluctuation is ±1 °C.

2.2. SHPB Experimental Principle

In the process of impact loading with the SHPB impact system, due to the low brittleness of rock specimens, the experiment must not only decouple the effects of the one-dimensional stress wave and strain rate, but also meet the assumptions of one-dimensional stress and stress homogenization.

The shock wave is transmitted along the incident rod, and a part of the reflection occurs after contacting the specimen, which generates the reflection wave. The reflection wave continues to be transmitted after contacting the specimen, and the transmission wave is generated in the transmission rod, which is finally absorbed by the absorption rod. The electrical signals generated by the incident wave $\varepsilon_I(t)$, reflected wave $\varepsilon_R(t)$, and transmitted wave $\varepsilon_T(t)$ are collected and processed by a dynamic strain gauge and finally

reflected in the oscilloscope. The dynamic stress $\sigma_s(t)$, dynamic strain $\varepsilon_s(t)$, and strain rate $\dot{\varepsilon_s}(t)$ of the specimen can be obtained by the three-wave method [18,19] (Equation (1)).

$$\begin{cases} \sigma_s(t) = \frac{EA}{2A_s}[\varepsilon_I(t) + \varepsilon_R(t) + \varepsilon_T(t)] \\ \dot{\varepsilon_s}(t) = \frac{C}{l}[\varepsilon_I(t) - \varepsilon_R(t) - \varepsilon_T(t)] \\ \varepsilon_s(t) = \int_0^t \dot{\varepsilon_s}(t)dt \end{cases} \quad (1)$$

2.3. Data Validity Verification

Similarly, when the experimental conditions satisfy the homogeneity assumption, the method shown in Section 2.2 (Equation (1)) can be used to test the validity of the experimental data. According to the relationship given in Equation (2), the reliability of the test data is verified by comparing the relationship between the transmitted wave, the incident wave, and the reflected wave, which is also called the stress balance test. In this experiment, all collected data were tested for stress balance. Figure 3 shows a typical test curve for stress equalization during the experiment.

$$\varepsilon_I(t) + \varepsilon_R(t) = \varepsilon_T(t) \quad (2)$$

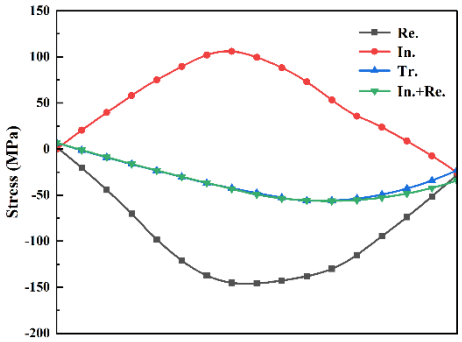

Figure 3. Typical test curve for stress equalization.

2.4. Experimental Materials and Scheme

The limestone specimens used in this work were taken from Katfang tin Mine, Honghe state, Yunnan Province. A cylindrical specimen with dimensions of Φ 50 mm × 40 mm (in Figure 4) was used, which is in accordance with the ISRM Suggested Methods [20].

Figure 4. Limestone specimen.

The heating rate is 10 °C/min. When the preset temperature of the device is reached, it remains constant for 2~3 h, and naturally cools down to room temperature. Figure 5 shows the heating temperature control curve. It is impossible to ensure that the heating rate of the rock specimen is completely consistent with the set heating rate in order to ensure that the specimen is damaged by the target temperature as a whole. Therefore, the

heating furnace is maintained at the target temperature once it is reached. Before cooling the test piece, the infrared thermometer is used to measure the surface temperature of the test piece. As there will be some error between the surface and internal temperatures of the test piece, we generally set the temperature slightly higher than the target temperature.

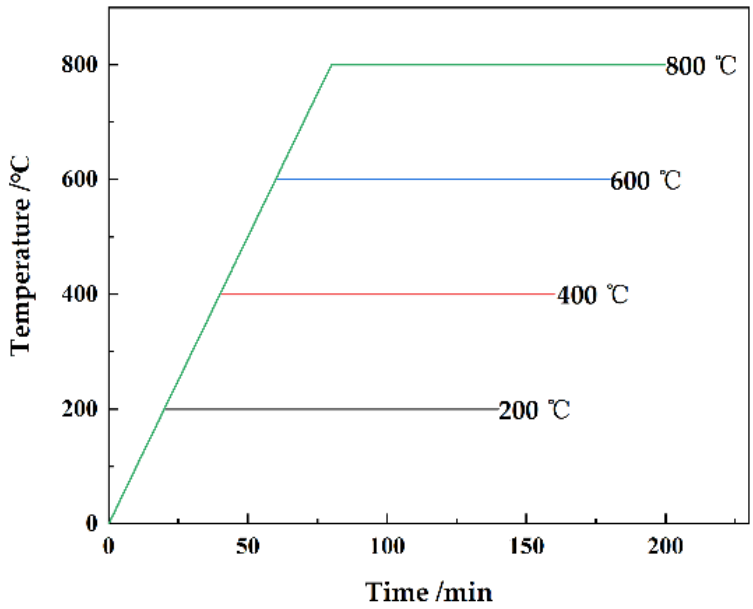

Figure 5. Heating temperature control curve.

In order to explore the influence of confining pressure and temperature damage on the dynamic mechanical properties of limestone specimens, the specimens were subjected to different temperatures and different confining pressures at loading impact velocities of 5.3 m/s and 8.6 m/s.

For comparison, the dynamic mechanical properties of the limestone specimens at room temperature were also tested at the corresponding impact rates without confining pressure. Three independent experiments were carried out under each working condition.

3. Experimental Results and Analysis

3.1. Experimental Results

The SHPB test system with a confining pressure device was utilized to study the effects of temperature (25 °C, 200 °C, 400 °C, 600 °C, and 800 °C), confining pressure (0.5 MPa, 1.5 MPa, and 2.5 MPa) and impact velocity (5.3 m/s and 8.6 m/s) on the dynamic mechanical properties of limestone.

The experimental results are shown in Table 1. In Table 1, a confining pressure of 0 MPa indicates that the dynamic impact experiments were carried out in a uniaxial state, and a temperature of 25 °C indicates that the dynamic impact experiments were performed at room temperature.

3.2. The Effects of High Temperature on Dynamic Mechanical Properties

Figure 6 presents the dynamic stress–strain curves of limestone specimens under different test conditions. At room temperature, the stress–strain curve can be divided into three stages: compaction stage, linear elastic stage, and destruction stage. The test results reported by Ping Qi et al. [21] also showed the same stages. The changing tendency of the uniaxial dynamic stress–strain curve for limestone after high-temperature treatment (200~800 °C) is similar to that at room temperature; the strength of the limestone first increases and then decreases with the increasing temperature.

Table 1. Mechanical properties of limestone under dynamic impact compression.

Impact Velocity (m/s)	Confining (MPa)	Temperature (°C)	Compressive Strength (MPa)	Peak Strain $\times 10^{-3}$	Elastic Modulus (GPa)
5.3	0	25	30.78	28.9	15.6
		200	33.68	28.1	16.83
		400	45.37	32.6	17.55
		600	38.56	34.5	22.03
		800	25.38	37.9	19.65
	0.5	25	33.35	2.72	7.65
		200	37.49	3.52	12.6
		400	46.42	4.66	14.38
		600	40.71	5.24	18.55
		800	32.72	5.51	14.7
	1.5	25	34.28	3.06	11.6
		200	39.13	5.48	20.11
		400	49.63	5.74	18.37
		600	41.06	4.62	28.5
		800	33.50	7.46	23.91
	2.5	25	46.06	4.11	11.39
		200	48.20	5.91	14.9
		400	53.56	7.88	24.16
		600	51.42	8.82	11.97
		800	37.39	8.89	13.66
8.6	0	25	39.63	48.8	19.72
		200	47.13	73.3	16.52
		400	48.20	48.8	16.33
		600	38.95	56.2	19.26
		800	39.73	54.2	15.24
	0.5	25	44.42	3.41	10.23
		200	53.20	6.03	14.44
		400	56.42	6.31	13.31
		600	49.99	8.88	15.33
		800	39.73	9.31	18.47
	1.5	25	55.70	4.5	16.32
		200	59.99	7.97	21.56
		400	66.42	8.2	14.77
		600	45.19	8.87	10.57
		800	43.63	10.91	23.11
	2.5	25	62.136	3.76	11.31
		200	68.778	5.31	18.78
		400	71.778	8.52	19.43
		600	49.280	6.16	17.18
		800	31.945	13.01	21.31

Figure 7 shows the relationship between the uniaxial dynamic compressive strength and temperature at an impact velocity of 5.3 m/s. Compared with the room temperature test condition, the dynamic compressive strength of limestone at 200 °C, 400 °C, and 600 °C is increased by 33.63%, 39.99%, and 19.87%, respectively. At 800 °C, the strength decreases by 19.54% and reaches the maximum value at 400 °C. This change is consistent with the pattern observed by Yin Tubing et al. when researching the impact of high temperatures on the dynamic compressive strength of granite specimens [22].

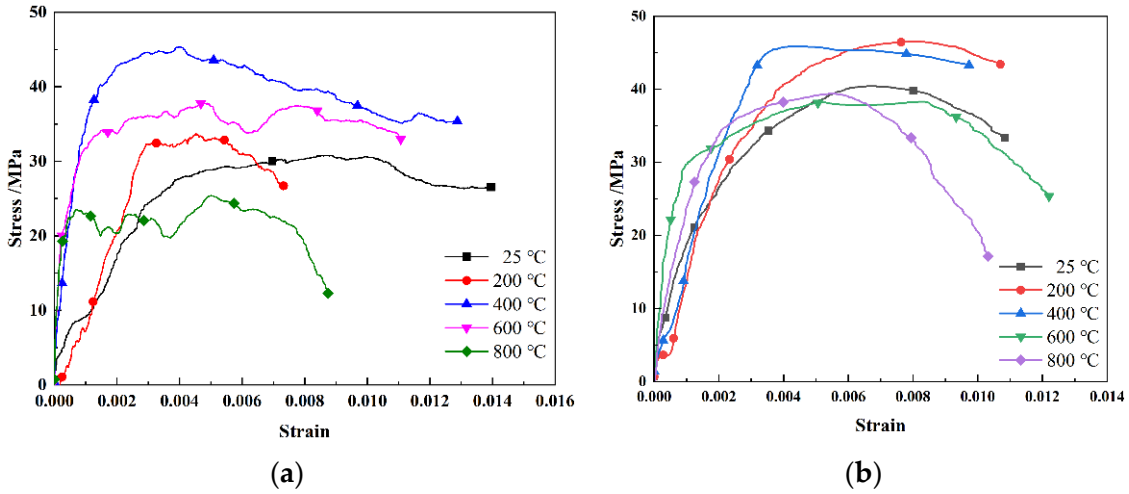

Figure 6. Dynamic stress–strain curves at different temperatures. (**a**) Impact velocity = 5.3 m/s; (**b**) Impact velocity = 8.6 m/s.

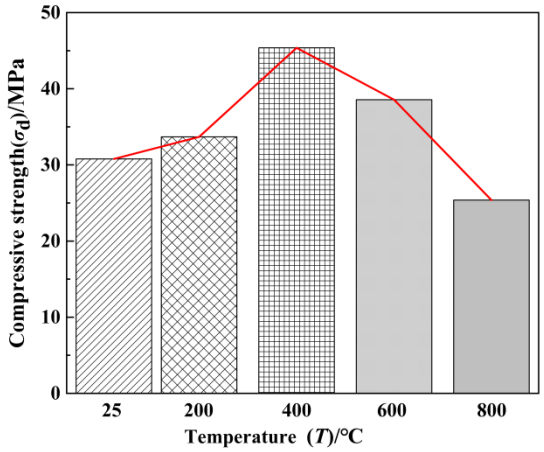

Figure 7. The relationship between uniaxial dynamic compressive strength and the temperature of limestone.

With the increase in temperature, the uniaxial dynamic compressive strength tends to first increase and then decrease, which shows that temperature has a significant effect on the uniaxial dynamic compressive strength of the limestone specimen. In the range of 25–400 °C, with the action of temperature, the water inside the specimen evaporates, the internal particles expand, and the internal pores close [23]. Hence, the temperature exerts a strengthening effect on the limestone. In addition, the increase in temperature contributes to the growth of limestone strength. When the temperature rises to 400 °C, the water inside the specimen completely evaporates, and the internal particles fully expand; at this point, the strengthening effect of the temperature on the uniaxial dynamic compressive strength of the limestone specimen is maximized. In the range of 400–600 °C, the internal particles of the limestone specimen continue to expand and squeeze each other, and the internal pores are basically closed. New pores and microcracks are generated inside the specimen [24]; at this time, the strengthening effect is still present (relative to room temperature of 25 °C), but it continuously decreases with the increasing temperature and reaches a minimum when the temperature is 400 °C. When the temperature exceeds 600 °C, the continuous development of internal pores and microcracks caused by the expansion of internal particles directly affects the dynamic compressive strength of the limestone specimen; at this time, the temperature generates a weakening effect on the uniaxial dynamic compressive strength of limestone (relative to room temperature of 25 °C). Furthermore, the weakening effect gradually increases as the temperature continues to rise.

3.3. The Effects of Confining Pressure on the Dynamic Mechanical Properties of Limestone after High-Temperature Treatment

Figures 8–10 show the dynamic stress–strain curves of limestone under different confining pressures at impact velocities of 5.3 m/s and 8.6 m/s after high-temperature treatment. Under the action of confining pressure, the peak stress in the limestone increases to different extents depending on the temperature. Moreover, the slope of the stress–strain curve changes accordingly. For temperatures lower than 400 °C, the peak of the curve shifts to the left as the temperature rises; in other words, the slope continuously increases. When the temperature exceeds 400 °C, the peak shifts to the right as the temperature rises; that is, the slope constantly decreases.

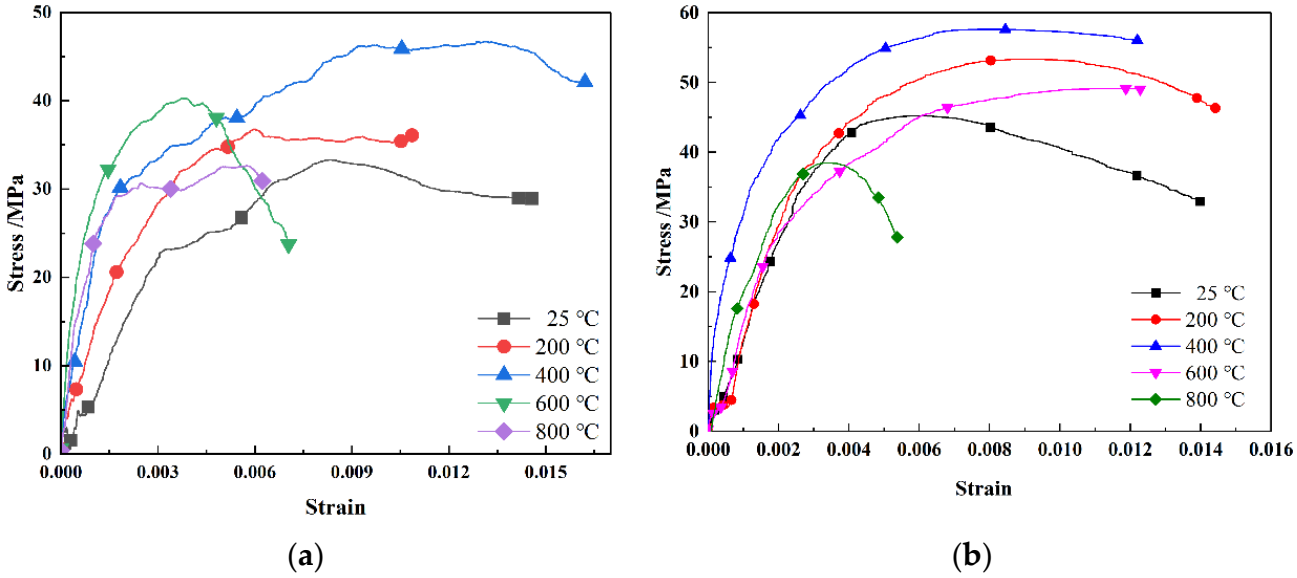

Figure 8. Dynamic stress–strain curve for a confining pressure of 0.5 MPa. (**a**) Impact velocity = 5.3 m/s; (**b**) impact velocity = 8.6 m/s.

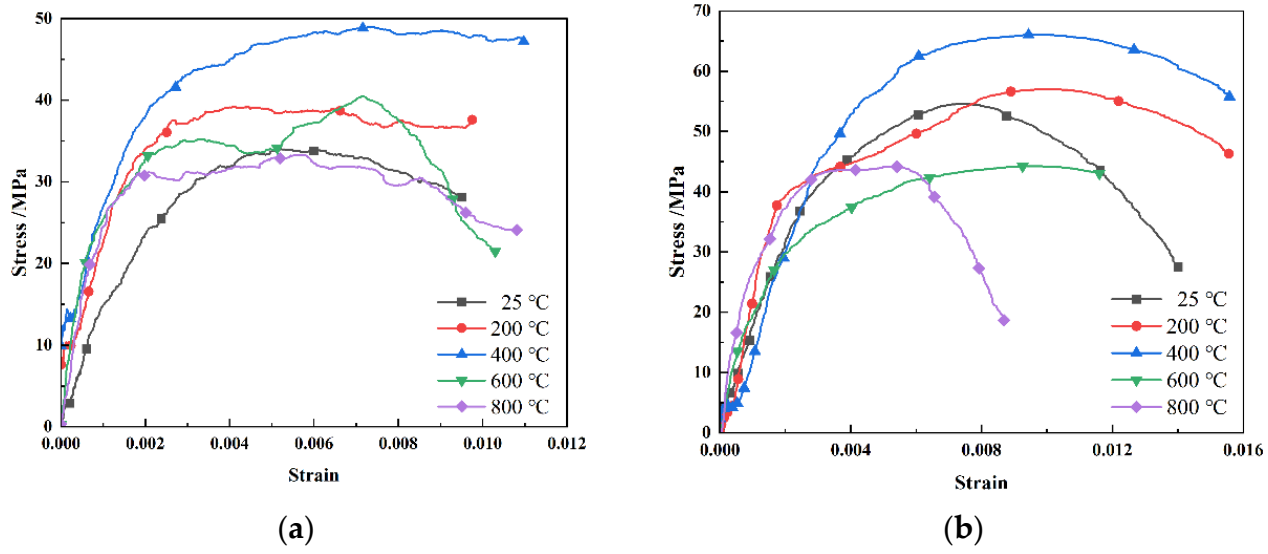

Figure 9. Dynamic stress–strain curve for a confining pressure of 1.5 MPa. (**a**) Impact velocity = 5.3 m/s; (**b**) impact velocity = 8.6 m/s.

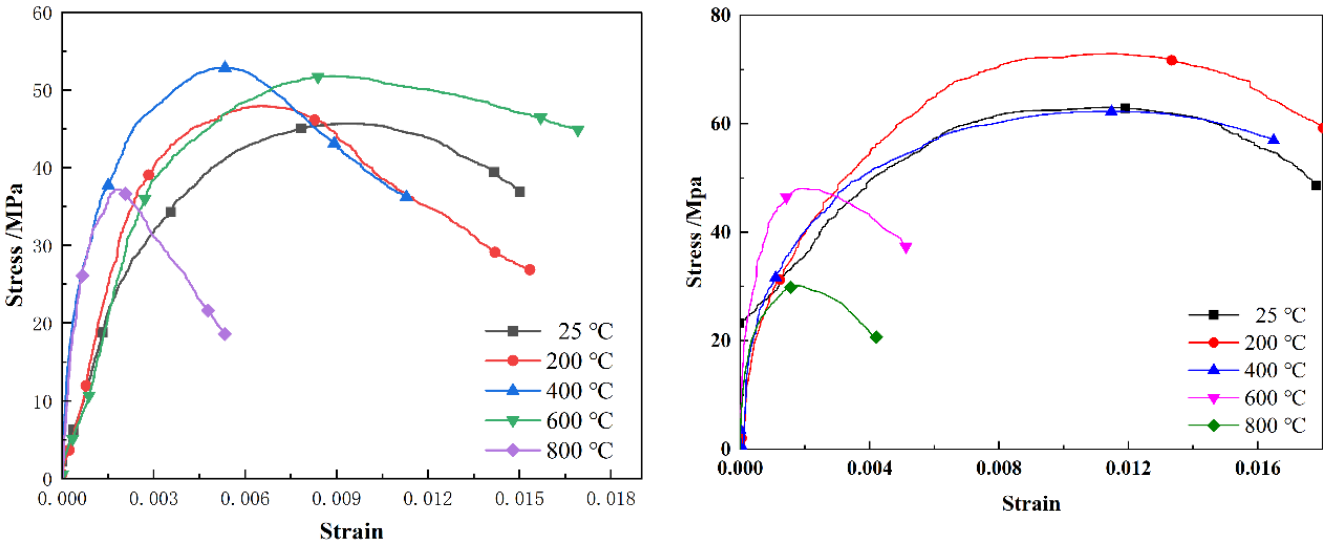

Figure 10. Dynamic stress–strain curve for a confining pressure of 2.5 MPa. (**a**) Impact velocity = 5.3 m/s; (**b**) impact velocity = 8.6 m/s.

The strength measurements of limestone subjected to different temperatures (25–800 °C) and different confining pressures (0 MPa, 0.5 MPa, 1.5 MPa, and 2.5 MPa) were used to draw the relationship curve between the dynamic compressive strength (σ_d) and confining pressure (σ_3) for different temperatures (T). Figure 11 shows that under different confining pressures, the effect of temperature on the strength of limestone is consistent with that without a confining pressure. As the temperature increases, the dynamic compressive strength of limestone first increases and then decreases. With the increase in confining pressure, the dynamic compressive strength also increases. A certain degree of positive correlation is observed, and it reaches the peak at a temperature of 400 °C and confining pressure of 2.5 MPa. According to the test results, high-temperature damage can affect the dynamic compressive strength by influencing the internal structure of the limestone specimen, while the confining pressure impacts the strength by affecting the tensile strength [25]. When both temperature and confining pressure act on the limestone specimen, the confining pressure enhances the temperature damage.

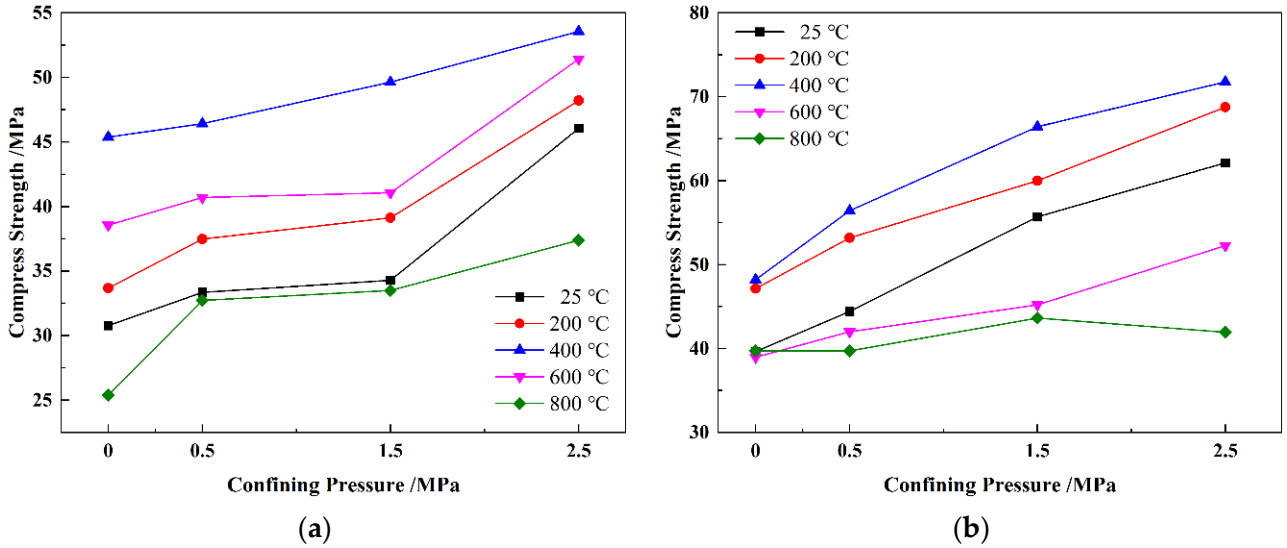

Figure 11. Dynamic compressive strength of limestone under different confining pressures after high-temperature treatment. (**a**) Impact velocity = 5.3 m/s; (**b**) impact velocity = 8.6 m/s.

3.4. The Dynamic Damage Constitutive Model for Limestone under the Action of Confining Pressure after High-Temperature Treatment

As the rock material, the limestone specimen can be regarded as a combination of a large number of differential elements; furthermore, it is also characterized by large numbers of pores and microcracks. Under naturally occurring conditions, these differential elements and internal pores and microcracks are distributed irregularly and unevenly. Therefore, the differential elements of rock can be assumed to be a parallel structure of viscous element λ and damage element D (Figure 12), and the following hypotheses can be made:

i. The impact of the acceleration of gravity on the constitutive relation of rock can be neglected;
ii. The damage and viscosity of the rock's differential element and the performance of the elastomer can be considered isotropous;
iii. Before the occurrence of damage, the differential element shows elastic properties and satisfies Hooke's Law;
iv. The constitutive relation of the viscous element satisfies the following:

$$\sigma = \eta \frac{d\varepsilon}{dt} \tag{3}$$

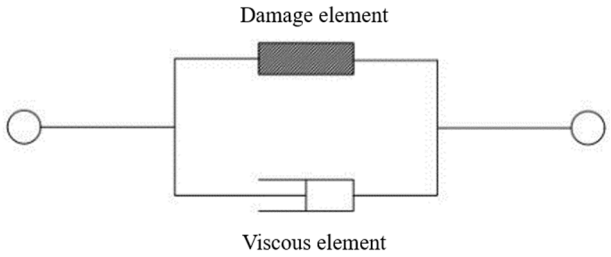

Figure 12. Differential element model.

v. The strength of the differential element has a Weibull distribution [26]; i.e., the density function satisfies the following:

$$\varphi\ (\mathrm{F}_0)\ = \frac{\mathrm{m}}{F_0}\left(\frac{F}{F_0}\right)^{m-1} \exp\left[-\left(\frac{F}{F_0}\right)^{m}\right] \tag{4}$$

The damage induced by the cumulative stress–strain and temperature is caused by effects on the internal structure of limestone. Therefore, when considering the internal damage of limestone due to the effects of the impact load and temperature, the impact load damage and the internal damage caused by temperature should be considered individually.

The analysis of the thermal damage of rock should factor in the influence of the internal material at the damaging temperature over a certain amount of time. From the perspective of wave velocity and modulus of elasticity, reference [27] presented a thermal damage model of different rocks. Given the need to include the stress–strain correspondence in this analysis, the elastic modulus representation was selected to characterize the thermal damage of limestone, as follows:

$$D_T = \frac{\Delta E}{E_0} = 1 - \frac{E_T}{E_0} \tag{5}$$

where D_T is the thermal damage to the limestone specimen under different temperatures, ΔE is the difference in elastic modulus among different temperatures and room temperature, and E_0 is the elastic modulus of limestone at room temperature.

The damage caused by the impact load effect is the result of the cumulative process of the internal stress–strain of the rock. The method in reference [28] expresses the damage

of rock by statistically representing the degree of destruction of the internal differential element, as follows:

$$D_M = \frac{N_t}{N} \tag{6}$$

where D_M refers to the damage variable, and N_t and N indicate the failure number and sum, respectively, of differential elements in the rock under certain conditions.

According to the assumption of the density function of the differential element in the basic hypothesis, an interval of random variation of some differential element (assuming that $[\varepsilon, \varepsilon + d\varepsilon]$) is utilized to represent the tendency of the damage variable to change with the stress state. Then, the number of damaged differential elements in a certain state can be represented as follows (Equation (7)):

$$N_t(\varepsilon) = \int_0^{\varepsilon} N\varphi(\varepsilon)d\varepsilon \tag{7}$$

Equations (4) and (7) can be substituted in Equation (6) to obtain the damage equation of limestone due to the impact load, as follows:

$$D_M = \frac{N_t(\varepsilon)}{N} = 1 - \exp\left[-\left(\frac{F}{F_0}\right)^m\right]. \tag{8}$$

The relation among the total damage D, thermal damage D_T, and load damage D_M can be expressed according to Equation (9) [29]. D_T and D_M can be substituted accordingly to obtain the expression of the general damage variable D, which is expressed by Equation (10):

$$D = D_T + D_M - D_T D_M. \tag{9}$$

$$D = 1 - \frac{E_T}{E_0}\exp\left[-\left(\frac{F}{F_0}\right)^m\right]. \tag{10}$$

Based on the D-P model [30], the strength of the differential element of limestone can be expressed by Equation (11):

$$F = \alpha_0 I_1 + \sqrt{J_2} \tag{11}$$

where α_0 is the coefficient related to the internal friction angle of limestone. I_1 and J_2 relate to the stress state of the differential element, and the corresponding expressions are shown in Equations (12) and (13).

$$I_1 = \sigma_1' + \sigma_2' + \sigma_3'. \tag{12}$$

$$J_2 = \frac{1}{6}\left[(\sigma_1' - \sigma_2')^2 + (\sigma_1' - \sigma_2')^2 + (\sigma_2' - \sigma_3')^2\right]. \tag{13}$$

where σ_1', σ_2', and σ_3'. are the effective stress received from different directions of various differential elements, as expressed by Equation (14):

$$\sigma_i' = \sigma_i(1 - D) \tag{14}$$

As shown in Figure 10, the stress obtained by the differential element of limestone is the sum of two parallel separations. The following relation should be satisfied for the two-fission strain of the differential element strain:

$$\sigma = \sigma_a + \sigma_b \tag{15}$$

$$\varepsilon = \varepsilon_a = \varepsilon_b \tag{16}$$

According to Hooke's Law, the strain of the elastic material and its corresponding stress state have a linear relationship [31,32]; furthermore, under confining pressure, the limestone receives equal radial force from all directions ($\sigma_2 = \sigma_3$). Then, ε_1 can be obtained as follows:

$$\varepsilon_1 = E^{-1}(\sigma_1' - 2\mu\sigma_2') \tag{17}$$

where μ is the Poisson's ratio of limestone.

Equation (14) can be substituted into Equation (17), resulting in the following:

$$\varepsilon_1 = E^{-1}(1-D)(\sigma_1 - 2\mu\sigma_2) \tag{18}$$

Then, the following can be deduced:

$$\sigma_1 = \varepsilon_1 E(1-D)^{-1} + 2\mu\sigma_2 \tag{19}$$

The dynamic constitutive equation of the differential structure of limestone under confining pressure after high-temperature treatment can be obtained by combining Equations (10), (11), (15) and (19), which is as follows:

$$\sigma = \varepsilon \frac{E_T{}^2}{E_0} \exp\left[-\left(\frac{F}{F_0}\right)^m\right] + 2\mu\sigma_2 + \eta\frac{d\varepsilon}{dt} \tag{20}$$

In Equation (20), F_0 and m are unknown parameters in the Weibull distribution function. Under the uniaxial loading condition, that is, when the confining pressure is 0 MPa ($\sigma_2 = \sigma_3 = 0\ MPa$), the peak of the stress–strain curve, namely, σ_{max} and ε_{max}, can be obtained; then, the relation can be expressed in Equation (21):

$$\frac{d\sigma_{max}}{d\varepsilon_{max}} = 0 \tag{21}$$

By taking the derivative of Equation (22) with respect to ε and substituting Equations (11) and (21) accordingly to solve for F_0 and m, the following is obtained:

$$F_0 = \left(\alpha_0 + \frac{1}{\sqrt{3}}\right) E\varepsilon m^{\frac{1}{m}} \tag{22}$$

$$\mathrm{m} = \frac{1}{\ln\left(E_T^2\varepsilon_D\right) - \ln\left(E_0\sigma_D - E_0\eta\frac{d\varepsilon}{dt}\right)} \tag{23}$$

Figure 13 compares the experimental results obtained under the uniaxial loading condition (confining pressure = 0 MPa) and under a confining pressure of 2.5 MPa.

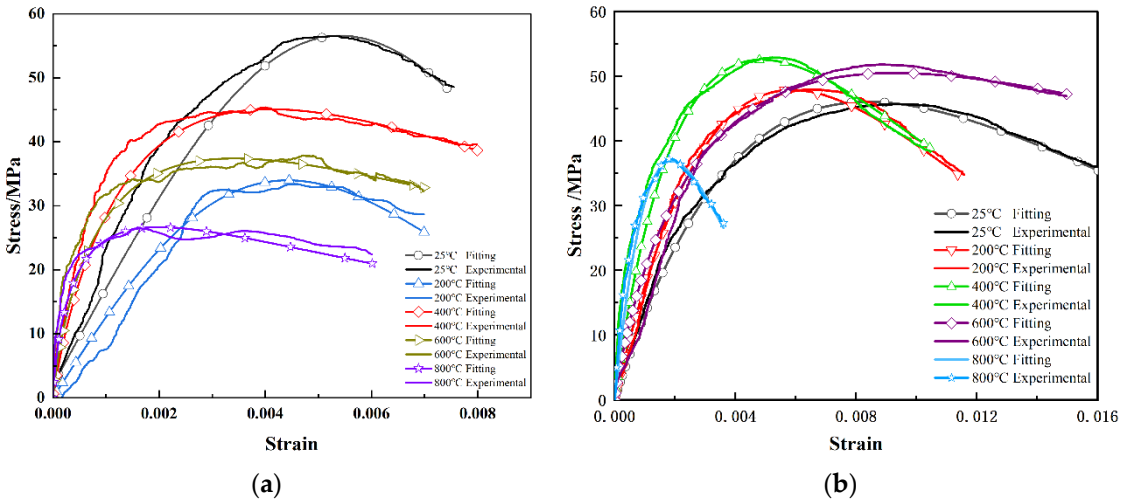

(**a**) (**b**)

Figure 13. Fitting of the dynamic damage constitutive model. (**a**) Confining pressure = 0 MPa; (**b**) confining pressure = 2.5 MPa.

Figure 13 shows the dynamic stress–strain curve established using the dynamic damage constitutive model of limestone after high-temperature treatment compared with the SHPB experimental results for limestone under different experimental conditions. The

changing tendency based on the model is almost identical to that of the actual laboratory experiment. The following characteristics apply to the fitted model:

The model can effectively express the change of "compaction" and "elastic" stages, in which failure occurs in the limestone specimen under the action of temperature, impact load, and confining pressure in various test conditions.

The model can effectively represent the dynamic compressive strength, peak stress, and elastic modulus of the limestone specimen under various test conditions.

In terms of the characterization of "failure" and "post-peak" stages in the dynamic failure process, the model results have certain differences from the laboratory test results. The model can be utilized to conduct research on the dynamic damage state of limestone under the action of confining pressure after high-temperature treatment. A laboratory experiment should be carried out with respect to the change features of the "post-peak" stage.

4. Conclusions

A high-temperature SHPB system was adopted to conduct dynamic compression tests on a limestone specimen under different confining pressures after being heated to different temperatures and naturally cooled to room temperature. Research on the SHPB test and dynamic damage constitutive model of limestone under the action of both confining pressure and temperature was carried out. The major conclusions are as follows:

The uniaxial dynamic stress–strain curve of limestone subjected to high temperatures has an almost identical changing pattern to the one at room temperature. The temperature can significantly impact the dynamic compressive strength of limestone, with a trend of first strengthening and then attenuating as the temperature rises.

After applying the confining pressure, the dynamic stress–strain curve of the limestone showed a consistent tendency with that in the uniaxial state. Through the limitation of lateral deformation, the confining pressure increased the dynamic compressive strength of the limestone. It also intensified the impact of temperature on the dynamic mechanical properties of limestone after high-temperature treatment. With the increase in confining pressure, the dynamic compressive strength also increased, reaching a maximum value at a temperature of 400 °C and confining pressure of 2.5 MPa.

A dynamic damage constitutive equation of limestone under the action of confining pressure after high-temperature treatment was established. According to comparisons with the experimental results, the model can reflect the relation among temperature, dynamic strength, strain, confining pressure, and strain rate under the action of confining pressure on the heated limestone.

Author Contributions: L.L. and W.S. designed the experiments; R.L. and H.Q. carried out the experiments; L.L. analyzed the experimental results. R.L. analyzed data and developed the analysis tools. W.S. and L.L. wrote the manuscript. All authors have read and agreed to the published version of the manuscript.

Funding: This research was funded by the National Natural Science Foundation of China (grant nos. 11862010 and 51964023).

Data Availability Statement: The data used to support the findings of this study are included within the article.

Conflicts of Interest: The authors declare no conflict of interest.

References

1. Xie, H.P.; Zhou, H.W.; Xue, D.J.; Wang, H.W.; Zhan, R.; Gao, F. Research and thinking on deep mining and limit mining depth of coal. *J. China Coal Soc.* **2012**, *37*, 535–542.
2. Xie, H.P. Research conception and prospect of "deep rock mechanics and mining theory". *Adv. Eng. Sci.* **2017**, *49*, 1–16.
3. Wang, S.M.; Sun, Q.; Qiao, J.W.; Wang, S.Q. Discussion on the geological guarantee of green mining of coal. *J. China Coal Soc.* **2020**, *45*, 8–15.
4. Zhao, G.Y.; Qiu, J.; Yuan, Z.; Pei, D.; Yang, L.; Pan, W. Discussion on evaluation method of green mining of metal. *Gold Sci. Technol.* **2020**, *28*, 169–175.

5. Mauko, A.; Fíla, T.; Falta, J.; Koudelka, P.; Rada, V.; Neuhäuserová, M.; Zlámal, P.; Vesenjak, M.; Jiroušek, O.; Ren, Z. Dynamic Deformation Behaviour of Chiral Auxetic Lattices at Low and High Strain-rates. *Metals* **2020**, *11*, 52. [CrossRef]
6. Fu, H.; Wang, X.; Xie, L.; Hu, X.; Umer, U.; Rehman, A.U.; Abidi, M.H.; Ragab, A.E. Dynamic Behaviors and Microstructure Evolution of Iron–nickel Based Ultra-high Strength Steel by Shpb Testing. *Metals* **2019**, *10*, 62. [CrossRef]
7. Klepaczko, J.R. Behavior of rock-like materials at high strain rates in compression. *Int. J. Plast.* **1990**, *6*, 415–432. [CrossRef]
8. Cherouat, A.; Borouchaki, H.; Jie, Z. Simulation of Sheet Metal Forming Processes Using a Fully Rheological-damage Constitutive Model Coupling and a Specific 3d Remeshing Method. *Metals* **2018**, *8*, 991. [CrossRef]
9. Lei, B.; Chen, G.; Liu, K.; Wang, X.; Jiang, X.; Pan, J.; Shi, Q. Constitutive Analysis on High-Temperature Flow Behavior of 3Cr-1Si-1Ni Ultra-High Strength Steel for Modeling of Flow Stress. *Metals* **2019**, *9*, 42. [CrossRef]
10. Li, X.B.; Gu, D.S.; Lai, H.H. Reasonable loading waveform in dynamic stress-strain map test of rock under impact load. *Explos. Shock. Waves* **1993**, *2*, 125–130.
11. Ping, Q.; Ma, Q.Y.; Lu, X.Y.; Yuan, W. Study on impact compression test of rock materials under passive confining pressure. *J. Vib. Shock.* **2014**, *33*, 55–59.
12. Xiao, M.; Ma, D.D.; Hu, D.W.; Zhou, H.; Chen, S.L.; Yu, Z.P.; Tan, X.F. Development and application of high temperature true triaxial test system in real time. *Chin. J. Rock Mech. Eng.* **2019**, *38*, 1605–1614.
13. Li, M.; Mao, X.; Cao, L.; Pu, H.; Lu, A. Influence of Heating Rate on the Dynamic Mechanical Performance of Coal Measure Rocks. *Int. J. Geomech.* **2017**, *17*, 04017020. [CrossRef]
14. Yin, T.; Li, X.; Xia, K.; Huang, S. Effect of Thermal Treatment on the Dynamic Fracture Toughness of Laurentian Granite. *Rock Mech. Rock Eng.* **2012**, *45*, 1087–1094. [CrossRef]
15. Fakhimi, A.; Azhdari, P.; Kimberley, J. Physical and Numerical Evaluation of Rock Strength in Split Hopkinson Pressure Bar Testing. *Comput. Geotech.* **2018**, *102*, 1–11. [CrossRef]
16. Mishra, S.; Chakraborty, T.; Matsagar, V. Dynamic Characterization of Himalayan Quartzite Using SHPB. *Procedia Eng.* **2017**, *191*, 2–9. [CrossRef]
17. Yin, Z.Q.; Li, X.B.; Jin, J.F.; He, X.Q.; Kun, D.U. Failure Characteristics of High Stress Rock Induced by Impact Disturbance Under Confining Pressure Unloading. *Trans. Nonferrous Met. Soc. China* **2012**, *22*, 175–184. [CrossRef]
18. Zhu, J.; Hu, S.; Wang, L. An Analysis of Stress Uniformity for Concrete-like Specimens During Shpb Tests. *Int. J. Impact Eng.* **2009**, *36*, 61–72. [CrossRef]
19. Ke, M.; Zhou, H. Dynamic Force Balance Analysis of SHPB System. *Met. Mine* **2010**, *39*, 27–30.
20. Zhang, Z.X.; Yu, J.; Kou, S.Q.; Lindqvist, P.A. Effects of High Temperatures on Dynamic Rock Fracture. *Int. J. Rock Mech. Min. Sci.* **2001**, *38*, 211–225. [CrossRef]
21. Ping, Q.; Wu, M.J.; Huan, Z.; Yuan, P. Experimental research on dynamic mechanical properties of sandstone under high-temperature condition. *Chin. J. Undergr. Space Eng.* **2019**, *15*, 691–698.
22. Yin, T.B.; Shu, R.H.; Li, X.B.; Pin, W.A.; Dong, L.J. Combined Effects of Temperature and Axial Pressure on Dynamic Mechanical Properties of Granite. *Trans. Nonferrous Met. Soc. China* **2016**, *26*, 2209–2219. [CrossRef]
23. Shu, R.H.; Yin, T.B.; Li, X.B.; Yin, Z.Q.; Tang, L.Z. Effect of heat-treatment on energy dissipation of granite under cyclic impact loading. *Trans. Nonferrous Met. Soc. China* **2019**, *29*, 158–169. [CrossRef]
24. Shi, L.; Xu, J. Effect of Strain Rate on the Dynamic Compressive Mechanical Behaviors of Rock Material Subjected to High Temperatures. *Mech. Mater.* **2015**, *82*, 28–38.
25. Yang, S.Q.; Yin, P.F.; Huang, Y.H.; Cheng, J.L. Strength, Deformability and X-ray Micro-ct Observations of Transversely Isotropic Composite Rock Under Different Confining Pressures. *Eng. Fract. Mech.* **2019**, *214*, 1–20. [CrossRef]
26. Kasyap, S.S.; Li, S.; Senetakis, K. Investigation of the Mechanical Properties and the Influence of Micro-structural Characteristics of Aggregates Using Micro-indentation and Weibull Analysis. *Constr. Build. Mater.* **2020**, *271*, 121509. [CrossRef]
27. He, A.; Wang, Z.; Bi, C. Experimental study on thermal damage characteristics and mechanism of Huashan granite. *Hydro-Sci. Eng.* **2018**, *1*, 95–101.
28. Krajcinovic, D.; Silva, M.A.G. Statistical Aspects of the Continuous Damage Theory—Science direct. *Int. J. Solids Struct.* **1982**, *18*, 551–562. [CrossRef]
29. Yin, T.; Wang, P.; Yang, J.; Li, X. Mechanical Behaviors and Damage Constitutive Model of Thermally Treated Sandstone Under Impact Loading. *IEEE Access* **2018**, *6*, 72047–72062. [CrossRef]
30. Zhou, J.; Yang, X.; Li, H. Numerical Solution for Mixed Mode Crack Propagation in Brittle Solids Combined with Finite Element Method and Failure Criteria. *Int. J. Mater. Prod. Technol.* **2012**, *45*, 96–107. [CrossRef]
31. Shi, X.; Zhou, W.; Chen, L.; Cai, Q.; Li, M.; Li, Z.; Luan, B. A New Unified Solution for Circular Opening Considering Different Strength Criteria and the Postpeak Elastic Strain Form. *Adv. Civ. Eng.* **2020**, *2020*, 1–21. [CrossRef]
32. Peng, J.; Tang, Z.C.; Hou, D. A Gsi-softening Model for Characterizing Strength Behavior of Thermally-damaged Rock. *Eng. Geol.* **2021**, *292*, 106251. [CrossRef]